Smurf1 regulates tumor cell plasticity and motility through degradation of RhoA leading to localized inhibition of contractility

Erik Sahai,[2] Raquel Garcia-Medina,[1] Jacques Pouysségur,[1] and Emmanuel Vial[1]

[1]Centre National de la Recherche Scientifique, UMR 6543, Centre Antoine Lacassagne, Nice 06189, France
[2]Tumour Cell Biology Laboratory, Cancer Research UK London Research Institute, London WC2A 3PX, England, UK

Rho GTPases participate in various cellular processes, including normal and tumor cell migration. It has been reported that RhoA is targeted for degradation at the leading edge of migrating cells by the E3 ubiquitin ligase Smurf1, and that this is required for the formation of protrusions. We report that Smurf1-dependent RhoA degradation in tumor cells results in the down-regulation of Rho kinase (ROCK) activity and myosin light chain 2 (MLC2) phosphorylation at the cell periphery. The localized inhibition of contractile forces is necessary for the formation of lamellipodia and for tumor cell motility in 2D tissue culture assays. In 3D invasion assays, and in in vivo tumor cell migration, the inhibition of Smurf1 induces a mesenchymal–amoeboid–like transition that is associated with a more invasive phenotype. Our results suggest that Smurf1 is a pivotal regulator of tumor cell movement through its regulation of RhoA signaling.

Introduction

Rho GTPases (e.g., RhoA, Rac1, and Cdc42) are key regulators of normal and tumor cell migration via the control of cell adhesion and cytoskeleton dynamics. In particular, RhoA is required through activation of its effector Rho kinase (ROCK) and the subsequent phosphorylation and activation of myosin light chain 2 (MLC2) to induce actomyosin contractility, driving translocation of the cell body and retraction of the rear (Hall, 1998; Ridley, 2001). Accordingly, the expression and activity of RhoA (and its close relative RhoC) and ROCK have been directly linked with invasion and metastasis (Clark et al., 2000; Sahai and Marshall, 2002; Croft et al., 2004; Hakem et al., 2005). However, the spatiotemporal activity of RhoA must be tightly regulated because it may also negatively influence cell migration and invasion by increasing stress fiber–dependent adhesions to the substrate (Cox et al., 2001; Vial et al., 2003). Therefore, it is important to identify the factors regulating RhoA activity and expression and their precise role in the processes of cell migration, invasion, and metastasis. In this context, it was recently shown that RhoA is locally targeted for proteasomal degradation at the cell leading edge by Smurf1, which is an E3-ubiquitin ligase of the C2-WW-HECT domain class. Smurf1 is recruited and activated at the leading edge by the Cdc42-activated polarity complex (PAR6-aPKC). This local degradation permits the correct extension of cellular protrusions and the establishment of cell polarity necessary for cell movement (Wang et al., 2003). We show that, in tumor cells, Smurf1 promotes lamellipodia formation and migration by specifically down-regulating RhoA activity and the downstream ROCK–MLC2 signaling pathway at the cell periphery. We next analyzed the potential function of Smurf1 in tumor invasion as a regulator of Rho signaling. We show that Smurf1 favors the protrusive, mesenchymal mode of invasion in 3D models and in vivo, in agreement with our 2D results. However, its inhibition does not block cell movement, but in contrast, induces the mesenchymal–amoeboid transition, which we demonstrate is associated with a more invasive phenotype. Thus, our work suggests that Smurf1, through its regulation of RhoA signaling, is a pivotal regulator of tumor cell movement in vitro and in vivo.

Correspondence to E. Vial: evial@unice.fr

Abbreviations used in this paper: MLC, myosin light chain; ROCK, Rho kinase; shRNA, short hairpin RNA.

The online version of this article contains supplemental material.

Results and discussion

To characterize the role of Smurf1 in MDAMB-231 breast cancer cells, we reduced its expression by using siRNAs or short hairpin RNAs (shRNAs) targeting different sequences in the *smurf1* gene (Fig. 1 a). siRNA (Fig. 1 b) or shRNA (Fig. 1 c) silencing was accompanied by cell rounding, a reduction in size, and a loss of membrane protrusions. Accordingly, silenced cells

The Journal of Cell Biology, Vol. 176, No. 1, January 1, 2007 35–42
http://www.jcb.org/cgi/doi/10.1083/jcb.200605135

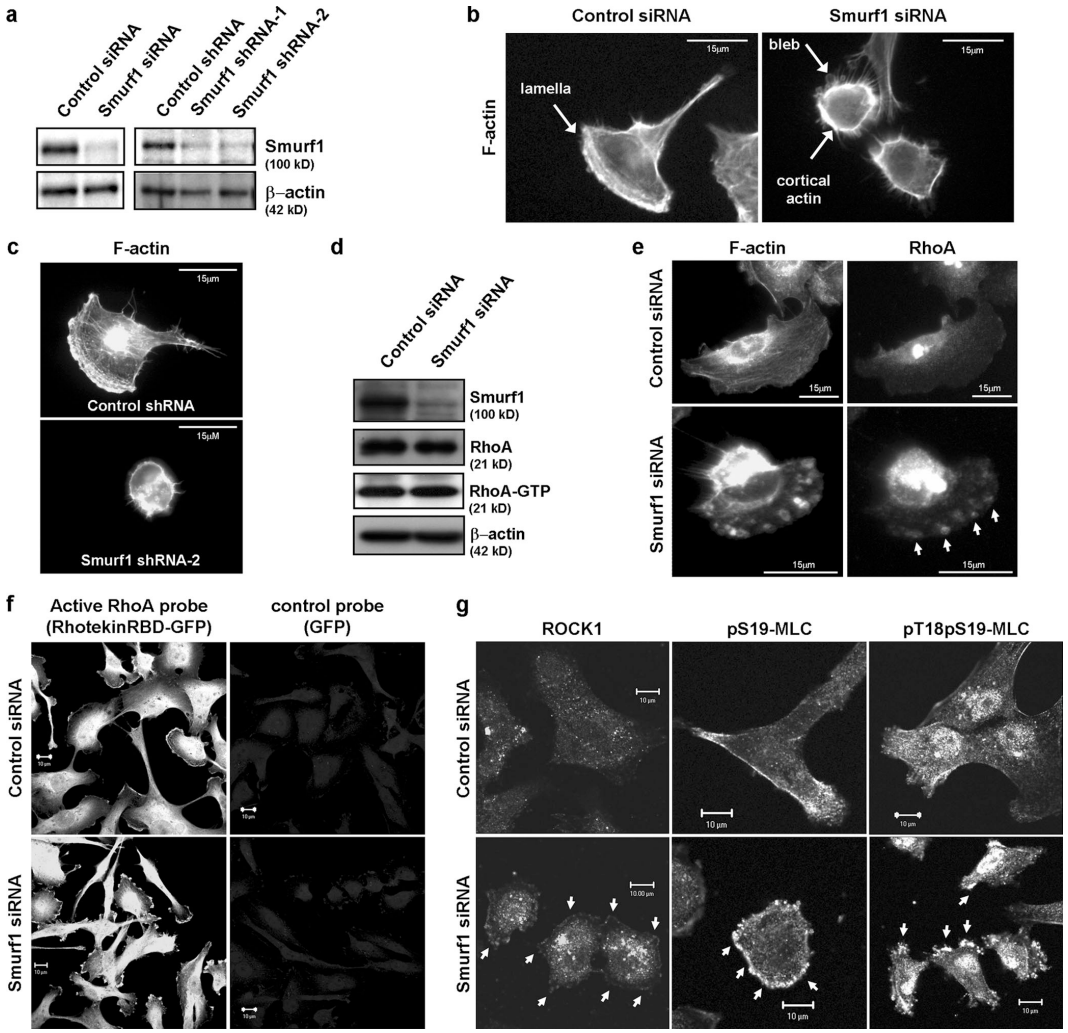

Figure 1. **Smurf1 is required for lamellipodia formation in carcinoma cells.** (a) Cell extracts from MDAMB-231 cells transfected with control and Smurf1-directed siRNAs and shRNAs were immunoblotted for the indicated proteins. (b) Control or Smurf1 siRNA–silenced MDAMB-231 cells were stained for F-actin. (c) Control or Smurf1 shRNA–silenced MDAMB-231 cells were stained for F-actin. (d) In control and Smurf1-silenced MDAMB-231 cells, levels of total and active pull-downed, GTP-bound RhoA, as well as the total amount of Smurf1 and β-actin, were determined by immunoblotting. (e) Control and Smurf1-silenced MDAMB-231 cells were stained for F-actin and RhoA. Arrows point to RhoA staining in blebs. (f) Level of active Rho was evaluated in control and Smurf1-silenced cells by analyzing GFP fluorescence after addition of a RBD(rhotekin)-GFP probe that only binds active GTP-bound Rho, or addition of a control GFP probe. (g) Control and Smurf1-silenced MDAMB-231 cells were stained for ROCK1, p(S19)-, and p(T18/S19)-MLC2. Arrows point to examples of peripheral ROCK and phospho-MLC staining.

displayed cortical actin staining, but the typical actin-rich lamellipodial extensions seen in control cells disappeared. In addition, some cells displayed bleblike structures typical of high Rho activity (Sahai and Marshall, 2003) with no effect on cell viability (unpublished data). These results confirm that Smurf1 expression is required for the formation of cellular protrusions; more precisely, we show in carcinoma cells that Smurf1 is required for the extension of lamellipodia. Although no substantial change in the overall accumulation of total RhoA or active GTP-bound RhoA could be observed in the Smurf1-silenced cells (Fig. 1 d), immunostaining studies showed a localized accumulation of RhoA in small areas at the cell periphery, particularly in some blebs (Fig. 1 e). The absence of a detectable change in the overall levels of RhoA might be explained by the presence of a large intracellular pool of RhoA unaltered by Smurf1 silencing. To test whether the pool of RhoA accumulated at the cell periphery is active, and therefore able to affect downstream signaling, we used an in situ probe for evaluation of the spatial Rho activity (Goulimari et al., 2005). Although the majority of control cells only showed an intracellular cytoplasmic active Rho localization (C3 treatment to inactive endogenous Rho proteins in control cells revealed that the staining of the nucleus and perinuclear region was nonspecific; unpublished data), most of the Smurf1-silenced cells displayed numerous dense patches of active Rho at the cell periphery, which is consistent with the accumulation of RhoA protein (Fig. 1 f). Furthermore, we observed that the activation of Rho was accompanied with a recruitment of ROCK1 at the cell periphery, together with an accumulation of phosphorylated, active MLC2 (Fig. 1 g). In an extension of the work of Wang et al. (2003), we conclude that Smurf1 down-regulates RhoA activity and the downstream ROCK–MLC2 signaling at the cell periphery.

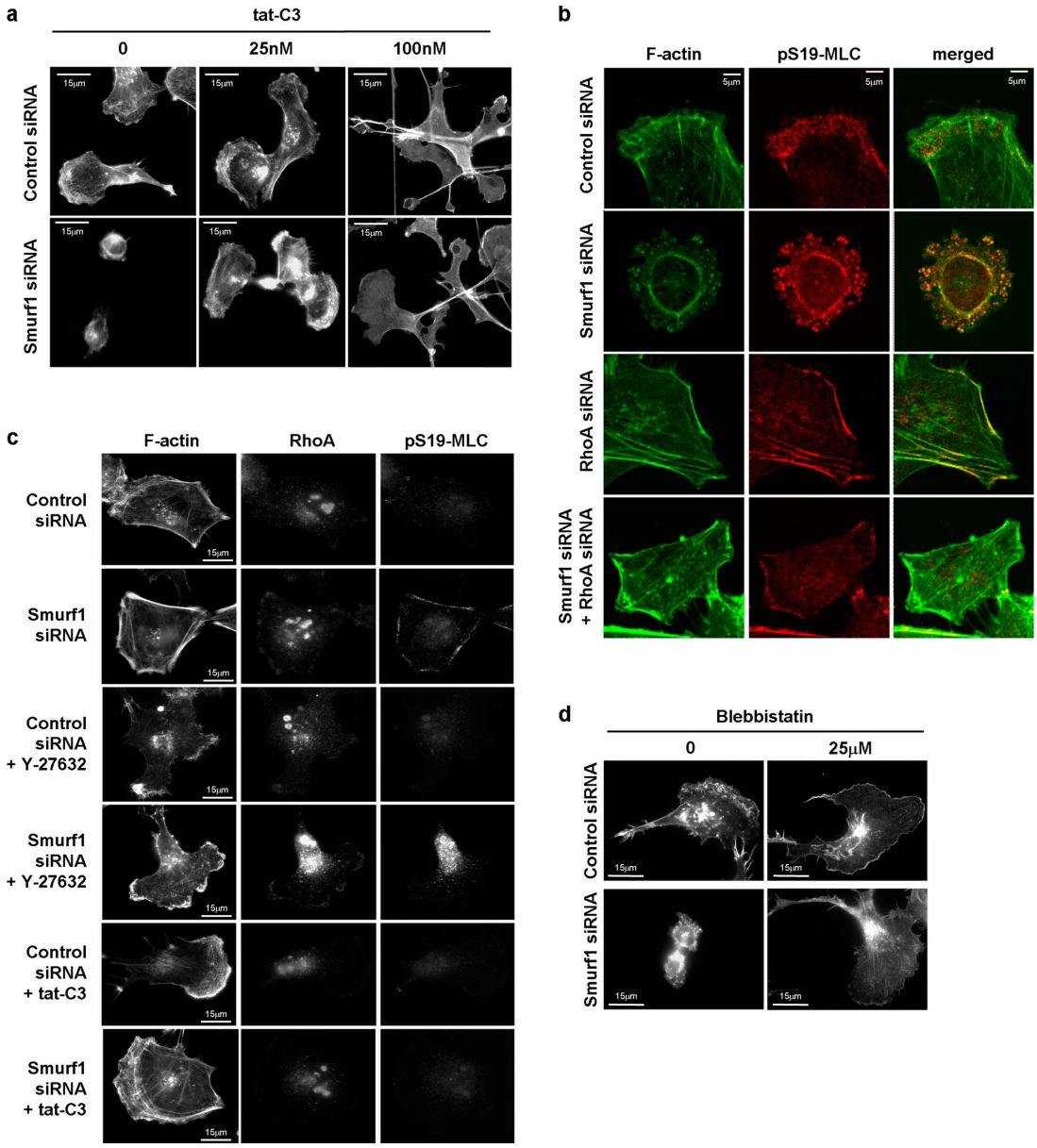

Figure 2. **The activation of peripheral RhoA–ROCK–MLC2 signaling in Smurf1-silenced cells is responsible for the loss of lamellipodia.** (a) Control or Smurf1-silenced MDAMB-231 cells were stained for F-actin; tat-C3 was added for 24 h. (b) Smurf1- and/or RhoA-silenced MDAMB-231 cells were stained for F-actin and p(S19)-MLC2. (c) Control or Smurf1-silenced MDAMB-231 cells were stained for F-actin, RhoA, and p(S19)-MLC2; 25 nM tat-C3 or 5 μM Y-27632 was added for 24 h. (d) Control or Smurf1-silenced MDAMB-231 cells were stained for F-actin; blebbistatin was added for 60 min.

To test whether this was responsible for the phenotype observed in the Smurf1-silenced cells, we first used a cell-permeable C3 toxin (tat-C3) known to ribosylate and inhibit Rho protein activity. As expected, lamellipodia were restored, and blebs and cortical actin disappeared in cells treated with a low dose of C3 (25 nM; Fig. 2 a). In both control and silenced cells, a high dose of C3 (>100 nM) resulted in the collapse of the actin cytoskeleton, which is consistent with a total inhibition of Rho activity and the formation of abnormal protrusions, as previously described (Worthylake and Burridge, 2003). RhoA is polyubiquitylated by Smurf1 on its conserved lysine 6 (Ozdamar et al., 2005), which is also present in RhoC. To test whether the phenotype of Smurf1-silenced cells is caused by a regulation of RhoA levels, but not of RhoC, we used siRNAs specifically targeting RhoA. We showed that the rounded phenotype and the appearance of pMLC-rich blebs are specifically antagonized by the RhoA siRNAs (Fig. 2 b); interestingly, we did not observe the more dramatic phenotype observed with 100 nM C3 treatment, suggesting that at high doses, C3 inhibits Rho GTPases in addition to RhoA. Similar experiments using siRNAs against RhoC did not produce any reversion of the Smurf1-silencing phenotype (unpublished data). Inhibition of ROCK using the synthetic inhibitor Y-27632 resulted in a phenotype similar to that observed with high doses of C3 (Fig. 2 c). Because MLC can also be activated by kinases other than ROCK (e.g., MLC kinase and MRCK), we showed that C3 and Y-27632

treatments also abolished the phosphorylation of MLC2 seen in Smurf1-silenced cells, indicating that it was Rho- and ROCK-dependent (Fig. 2 c). We next showed that blebbistatin, which is a nonmuscle myosin ATPase inhibitor, also rescued the effect of Smurf1 silencing (Fig. 2 d), suggesting that the absence of protrusion, the rounding, and the appearance of blebs are at least partially caused by an increase in peripheral actomyosin contractility. Importantly, we further confirmed the central role of Rho signaling by showing that Smurf1 silencing in tumor cells does not affect the other ubiquitylation targets of Smurf1, such as the SMAD proteins involved in the transcriptional response to TGFβ (Fig. S1 a, available at http://www.jcb.org/cgi/content/full/jcb.200605135/DC1; Izzi and Attisano, 2004) and the MEKK2–JNK signaling pathway (Fig. S1 b; Yamashita et al., 2005). Altogether, our work demonstrates that the activation of RhoA–ROCK–MLC2 signaling at the cell periphery observed in the Smurf1-silenced cells, and the consequent increase in actomyosin contractility, is responsible for the loss of lamellipodia and the formation of blebs.

To evaluate the consequence of these morphological modifications on the invasive phenotype, we first monitored the random motility of MDAMB-231 cells upon Smurf1 silencing. Cell migration was reduced by ∼80%; it was partially restored C3 and Y-27632 treatments (Fig. 3 a). These results, together with the regulation of Rho signaling, were reproduced in BE and HT1080 tumor cells (unpublished data). Consistently, cell migration was also inhibited by overexpression of two Smurf1-interfering mutants: Smurf1-C699A, which is deficient in its ubiquitin ligase activity (Wang et al., 2003), and Smurf1-ΔC2, which fails to localize at the plasma membrane (Fig. 3 b; Suzuki et al., 2002). As for Smurf1 silencing, both mutants induced cell rounding, loss of membrane protrusions, blebbing, and accumulation of RhoA at the cell periphery (Fig. 3 c). Notably, C3 and Y-27632 treatments in control cells did not significantly affect cell migration. One possibility is that in MDAMB-231 cells, the actomyosin contractility necessary for cell movement is also generated by the Cdc42–MRCK pathway (Wilkinson et al., 2005). These results indicate that RhoA–ROCK–MLC2 signaling is not essential for MDAMB-231 cell movement in 2D, and, more importantly, that it needs to be specifically inhibited by Smurf1 at the cell periphery to allow the formation of protrusions and tumor cell migration. The lowering of myosin-dependent contractile signals at the cell edge is probably required to diminish the local tension and adhesive forces, allowing the Rac-driven extension of the lamellipodium. The localized nature of Smurf1 activity permits it to maintain the intracellular Rho–ROCK–MLC2 activity, which is likely to be required for contraction of the cell body and retraction of the rear (Fig. S2, available at http://www.jcb.org/cgi/content/full/jcb.200605135/DC1).

In contrast to the situation in 2D tissue culture, there are several mechanisms of tumor cell migration in vivo and in 3D models of invasion (Friedl and Wolf, 2003; Sahai, 2005). The protease-dependent mesenchymal mode of movement needs low activities of RhoA and ROCK to allow, as seen in 2D, the extension of Rac-dependent protrusions at the front (Vial et al., 2003). On the contrary, the second main mode of motility, called amoeboid, is protease independent, but depends on high activities of Rho, ROCK, and MLC2 to generate cortical contractile forces used for matrix deformation; it does not extend protrusions and it is associated with a more rounded morphology (Sahai and Marshall, 2003; Wyckoff et al., 2006). Importantly, cancer cells can switch from one mode of movement to another, depending on the 3D microenvironment. Rho signaling is pivotal because its blockade induces the mesenchymal–amoeboid transition and, conversely, its constitutive activation leads to a conversion to the amoeboid mode of movement. To analyze the role of Smurf1 in invasion, we first studied cell motility in 3D Matrigel matrices in vitro. We used the previously described

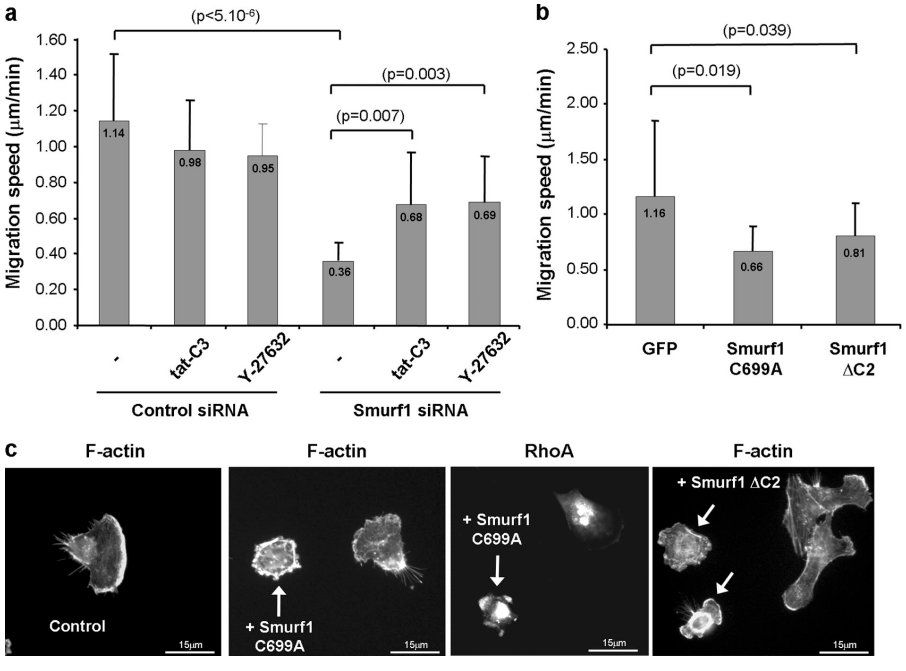

Figure 3. **Smurf1 is required for tumor cell migration in 2D.** (a) Random migration speed of control or Smurf1-silenced MDAMB-231 cells was averaged over a 6-h period of cell tracking by phase-contrast time-lapse microscopy. 10 μM Y-27632 or 0.5 μM tat-C3 was added to the medium 24 h before analysis. $n = 3$; mean ± the SD. At least 25 cells were analyzed in each experiment. P values of *t* test are indicated. (b) 48 h after transfection of p-EGFP-N1 alone or together with interfering Smurf1-C699A and Smurf1-ΔC2 mutants, EGF-expressing MDAMB-231 cells were tracked over a 6-h period by time-lapse microscopy for analysis of random migration. $n = 2$; mean ± the SD; at least 25 cells were analyzed in each experiment; P values of *t* test are indicated. (c) Alternatively, transfected cells were fixed and stained for F-actin and RhoA. Arrows indicate transfected cells.

mesenchymal BE colon carcinoma cells, which display low RhoA activity, and the amoeboid A375m2 melanoma cells with high RhoA activity (Figs. 4, a and b; Sahai and Marshall, 2003). When Smurf1 was silenced in A375m2 cells, the morphology and the invasion of the 3D matrix were unaltered, as most of the cells kept the rounded phenotype (Fig. 4 c). In contrast, silencing of Smurf1 in BE cells resulted in a dramatic transition from the mesenchymal to the amoeboid morphology and mode of invasion, which was partially reversed by treatment with Y-27632. These results suggest that in cancer cells, Smurf1 expression, through the local down-regulation of RhoA–ROCK activity and the formation of cellular protrusions, favors the mesenchymal mode of invasion in 3D.

We next asked if Smurf1 would also be required for the mesenchymal morphology in an in vivo tumor environment and what would be its impact on invasion. To trigger stable and long-term inhibition of Smurf1 in vivo, we generated BE tumor cell lines stably expressing GFP and shRNAs against Smurf1 (Fig. 5 a). As seen with BE and MDAMB-231 cells transiently expressing the siRNAs against Smurf1, these clones showed a reduced cell motility in 2D and displayed the amoeboid phenotype in Matrigel (unpublished data). BE clones were grown as subcutaneous tumors in nude mice, and multiphoton intravital microscopy was used on living animals to analyze tumor cell morphology and movement. In vivo, BE cells expressing the control shRNA had an overall elongated morphology, whereas cells expressing the Smurf1 shRNAs were mostly rounded, confirming our in vitro observations (Fig. 5 b). In agreement, in the control tumors, time-lapse intravital imaging showed that the moving cells used the mesenchymal mode of motility by extending protrusions at the front. Interestingly, only a minority of cells was migrating, but even the static cells presented the elongated morphology (Fig. 5 c; Video 1), indicating that additional factors intrinsic to the tumor microenvironment are required to promote cell movement. In the Smurf1-silenced tumors, all cells were rounded, particularly those migrating, thus confirming that they were using the amoeboid motility (Fig. 5 c; Video 2). These data demonstrate that in tumors, Smurf1 favors the mesenchymal mode of invasion, and that its inhibition induces the mesenchymal–amoeboid transition in agreement with the activation of Rho-dependent contractile signals in 2D. Interestingly, although previous studies showed that the different modes of invasion and the plasticity between those were characterized and regulated by the general level of RhoA–ROCK–MLC2 activity in the cells (Sahai and Marshall, 2003; Wyckoff et al., 2006), our work shows that subtle changes at the cell periphery induced by Smurf1, which were undetectable at the biochemical level, are sufficient to induce the transition in the invasion strategies. Factors that can regulate either Smurf1 expression or its activity in the process of tumor development are therefore potential key elements in the plasticity of cancer cell invasion. This is important because the plasticity between the different modes of movement allows tumor cells to be highly adaptable to the dynamic microenvironment in cancer, and it might provide an escape mechanism to antiinvasive treatments (Friedl and Wolf, 2003).

Finally, we sought to analyze the impact of Smurf1 silencing on the efficiency of cell movement, invasion, and metastasis. Intravital analyses revealed that upon Smurf1 silencing there were approximately three times as many cells migrating, indicating that the transition to the amoeboid mode movement significantly increases cell motility in tumors (Fig. 5 d). Strikingly, although control cells were never seen in tumor vessels (blood or lymphatic), Smurf1-silenced amoeboid BE cells were

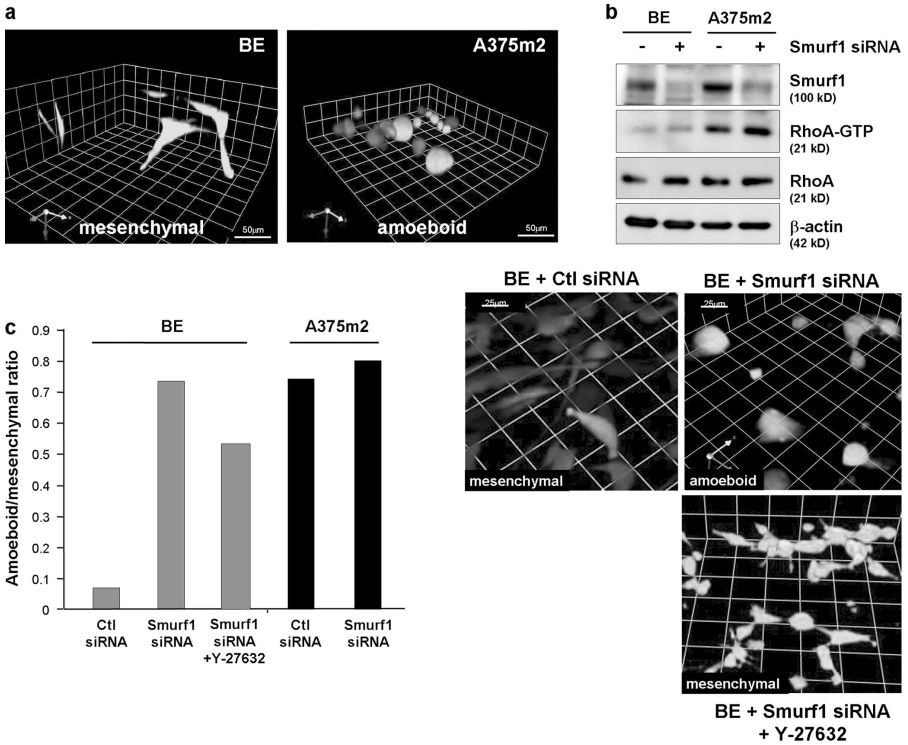

Figure 4. **Smurf1 silencing induces the mesenchymal–amoeboid transition in 3D matrices in vitro.** (a) BE and A375m2 cells expressing GFP and embedded within a thick 3D Matrigel matrix were imaged after fixation by capturing at least 30 confocal sections. These were subsequently reconstructed in 3D using Volocity imaging software. (b) Levels of total and active pull-downed, GTP-bound RhoA from control and Smurf1-silenced BE and A375m2 cells were determined by immunoblotting. (c) Control or Smurf1-silenced BE and A375m2 cells expressing GFP were allowed to invade a thick 3D Matrigel matrix for 96 h; for ROCK inhibition, 5 μM Y-27632 was added to the medium every day. Only cells that invaded a minimum of 10 μm inside Matrigel were scored as invasive and analyzed for morphology by confocal sectioning and 3D reconstruction. The ratio of amoeboid cells to mesenchymal cells is shown on the left, as well as representative 3D reconstructions. One representative experiment out of two is shown.

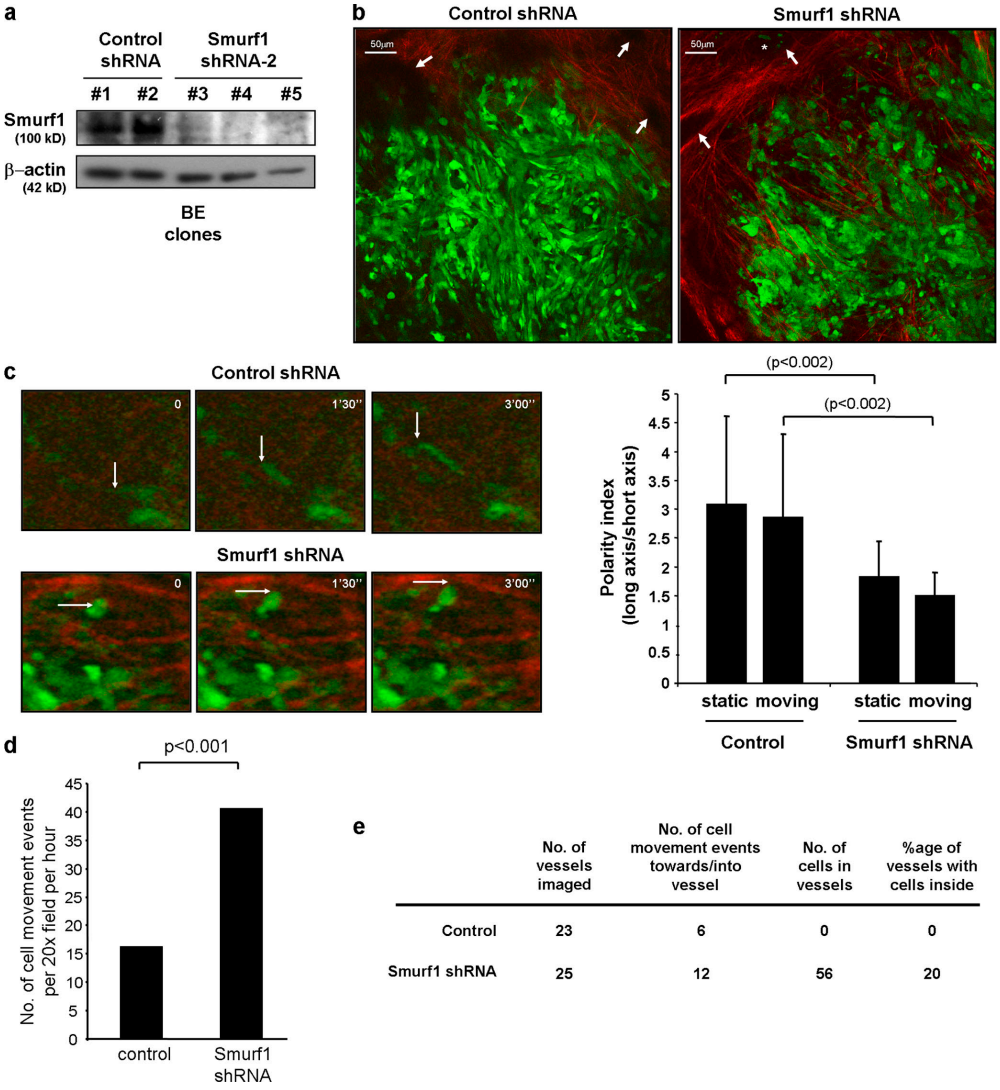

	No. of vessels imaged	No. of cell movement events towards/into vessel	No. of cells in vessels	%age of vessels with cells inside
Control	23	6	0	0
Smurf1 shRNA	25	12	56	20

Figure 5. **Smurf1 silencing induces the mesenchymal–amoeboid transition in vivo and increases invasion and intravasation.** (a) Cell extracts from independent BE clones stably expressing GFP and the control or Smurf1 shRNAs were immunoblotted for the indicated proteins. (b) Control and Smurf1-silenced BE-GFP clones were injected subcutaneously to form a tumor xenograft. Morphology of GFP-expressing tumor cells was analyzed in vivo using multiphoton intravital microscopy. Tumor cells are shown in green, and collagen fibers of the tumor stroma are shown in red. Arrows indicate tumor vessels; asterisk shows tumor cells in vessels. (c) Movement of tumor cells was imaged over time in vivo using multiphoton intravital microscopy (Videos 1 and 2). 90-s separated frames are shown (left). Movement of one individual tumor cell is indicated by an arrow. Polarity index (as an evaluation of the mesenchymal or amoeboid morphology) of static and moving tumor cells within the tumor is shown on the right. P values of *t* tests are indicated. (d) Cell motility was evaluated quantitatively by measuring the mean number of moving cells per microscope field in the control or Smurf1-silenced tumors. (e) The presence of tumor cells in vessels was imaged and quantified using intravital multiphoton microscopy (Video 3 and 4). Data are derived from analysis of 14 control BE tumor videos and 18 BE Smurf1 shRNA videos. Videos 1–4 are available at http://www.jcb.org/cgi/content/full/jcb.200605135/DC1.

often imaged in the vessels or intravasating (Figs. 5, b and e; Videos 3 and 4). The number of blood vessels was unaffected by Smurf1 silencing (Fig. S3). However, the growth of Smurf1-silenced or control subcutaneous tumors never resulted in the formation of visible distant metastases, indicating that in this model additional factors are needed for BE cells to efficiently metastasize. Nevertheless, to test whether Smurf1-silencing could also affect the later stages of cancer dissemination, we injected tumor cells directly into the tail vein of immunodeficient mice for measurement of lung metastases. As for the subcutaneous model, we found that BE cells did not readily metastasize and that Smurf1-silencing did not increase metastasis (unpublished data). Collectively, these data show that Smurf1 knockdown and the mesenchymal–amoeboid transition in tumors increases tumor cell motility and favors intravasation, but it is not sufficient to promote metastasis after cells have entered the vessels. Our results are in agreement with previous work (Wang et al., 2002), showing that mesenchymal cells often fragment when they enter the blood stream and that, instead, highly metastatic carcinoma cells efficiently crawl into the blood vessels by using the amoeboid locomotion. It is worth noting that the efficiency of tumor cell motility in 2D therefore does not necessarily reflect the invasive potential in vivo.

In conclusion, our work demonstrates that Smurf1, through the regulation of peripheral RhoA–ROCK–MLC2 signaling, is a key element of tumor cell motility and invasion in vitro,

as well as in vivo. Recent data have suggested that Smurf1 activity can be activated by TGFβ in normal epithelial cells to induce the degradation of RhoA at the tight junctions, leading to the dissolution of these cell–cell junctions and the subsequent TGFβ-dependent epithelial–mesenchymal transition (Ozdamar et al., 2005). We hypothesize that Smurf1 could be implicated in two crucial aspects of tumor progression in a Rho-dependent manner; in the first stages of the invasive progression, Smurf1 might be activated by TGFβ to disrupt normal epithelial organization (Ozdamar et al., 2005). In carcinomas that have lost their epithelial organization, such as those analyzed in this study, down-regulation of Smurf1 expression or activity would then increase motility. Investigation of the "Oncomine" resource (www.oncomine.org) shows that overall Smurf1 levels do not change greatly with tumor grade or prognosis; however, this is entirely consistent with our results, which indicate that reduction of Smurf1 facilitates cell motility and intravasation specifically, and not the entire metastatic process.

Materials and methods

Cell lines and plasmids

MDAMB-231 breast cancer cells, BE and LS174T colon carcinoma cells, A375m2 melanoma cells, and HT1080 fibrosarcoma cells were gifts from C.J. Marshall (Institute of Cancer Research, London, UK). Stable GFP-expressing clones were selected after transfection of pEGFP-N1 (CLONTECH Laboratories, Inc.). Cells were routinely maintained in DME supplemented with 10% FCS. cDNAs for the human Smurf1-interfering mutants Smurf1-C699A and -ΔC2 were gifts from J. Wrana (University of Toronto, Toronto, Canada). SBE4 reporter construct was a gift from B. Vogelstein (Johns Hopkins Oncology Center, Baltimore, MD). The truncated activated ROCK1 mutant ROCKΔ3 was described elsewhere (Sahai and Marshall, 2003). Transfections were carried out using Lipofectamine 2000 (Invitrogen) according to the manufacturer's recommendations.

Reagents and antibodies

Cell-permeable C3 (Tat-C3) was prepared as previously described (Sahai and Olson, 2006). Y-27632 was obtained from Tocris. Human TGFβ1 (R&D Systems) was a gift from E. van Obberghen-Schilling (Institute of Signaling Developmental Biology and Cancer, Nice, France) and was used at 1 ng/ml. Anisomycin was used at 0.5 μg/ml, and blebbistatin was used at 25 μM, for 60 min. Antibodies used were as follows: Smurf1 (Santa Cruz Biotechnology, Inc.); RhoA (Santa Cruz Biotechnology, Inc.); β-actin (Sigma-Aldrich); MYC (Cell Signaling Technology); phospho-JNK1/2 (Promega); phospho(Ser3)-cofilin (Cell Signaling Technology); ROCK1 (Santa Cruz Biotechnology, Inc.). Antibodies against phospho(Ser19)-MLC2 (Cell Signaling Technology), phospho(Thr18/Ser19)-MLC2 (Cell Signaling Technology), and phospho-LIMK (Cell Signaling Technology) were gifts from M. Olson (Cancer Research UK Beatson Institute for Cancer Research, Glasgow, UK). Secondary antibodies for immunofluorescence were obtained from Promega. The RBD(rhotekin)-GFP probe was a gift from R. Grosse (University of Heidelberg, Heidelberg, Germany) and was used as previously described (Goulimari et al., 2005).

siRNAs and shRNAs

Oligonucleotides were purchased from Dharmacon and Eurogentec. The siRNA sequences targeting human *smurf1* used were as follows: sense, CCGACACUGUGAAAAACACdTdT; antisense, GUGUUUUUCACAGUGUCGGdTdT. The RhoA siRNA sequences used were as follows: sense, GAACUAUGUGGCAGAUAUCUUdTdT; antisense, AAGAUAUCUGCCACAUAGUUCdTdT. The control oligonucleotides targeting the *Drosophila melanogaster hif1α* gene were gifts from E. Berra (Institute of Signaling Developmental Biology and Cancer, Nice, France) and were previously described (Berra et al., 2003). siRNAs were transfected using the Oligofectamine reagent (Invitrogen) according to the manufacturer's recommendations. For construction of the shRNA vectors targeting Smurf1, the targeted sequences in the human *smurf1* gene were 5′-TACGTCCGGTTGTATGTAA-3′ (shRNA-1) and 5′-TGAAGGAACGGTGTATGAA-3′ (shRNA-2). The corresponding oligonucleotides (sequences available upon request) were annealed and cloned into the shRNA-expressing vector pTER (van de Wetering et al., 2003). These vectors and a vector expressing a control shRNA (gift from E. Berra) were transfected into MDAMB-231 cells for transient expression of the shRNAs, or into BE cells for the generation of stable cell lines constitutively expressing the shRNAs. All the shRNA transfections were done using Lipofectamine 2000.

Immunoblotting, Rho pull-down assays, and immunocytochemistry

Whole-cell extracts were harvested in 1.5× Laemmli sample buffer, and immunoblotting was performed using standard procedures. RhoA pull-down assays were performed using GST-rhotekin, as previously described (Sahai et al., 2001); levels of total and active RhoA were revealed using a RhoA-specific antibody (Santa Cruz Biotechnology, Inc.). For immunofluorescence, cells were washed with PBS, fixed with 4% paraformaldehyde in PBS, and permeabilized with 0.2% Triton X-100 in PBS. After several PBS washes, cells were either stained for the actin cytoskeleton with Alexa Fluor 568–phalloidin (Invitrogen) or primary antibodies were added for 2 h; after several PBS washes, appropriate secondary antibodies conjugated to Alexa Fluor 488, 568, or 647 were added for 1 h; cells were mounted after several additional PBS washes and viewed using a microscope (Axiovert 200) with Plan Apochromat 63×/1.4 NA oil or Plan Neofluor 40×/1.3 NA oil objectives, a camera (HAL100), and Immersol medium with N_e = 1,518 (all from Carl Zeiss MicroImaging, Inc.).

Luciferase assays

For analysis of luciferase activity, transfected cells were lysed in 25 mM Tris-phosphate, pH 7.8, 2 mM DTT, 2 mM 1,2-diaminocyclohexane-*N,N,N′,N′*-tetraacetic acid, 10% glycerol, and 1% Triton X-100. Light emission was quantified using a luminometer (1450 Microbeta; Wallac) after addition of the luciferase substrate (20 mM Tricine, 1.07 mM $(MgCO_3)_4Mg(OH)_2.5H_2O$, 2.67 mM $MgSO_4$, 0.1 mM EDTA, 33.3 mM DTT, 0.27 mM coenzyme A, 0.47 mM luciferin, and 0.53 mM ATP). As a control, β-galactosidase activity was quantified in the lysate using the Galacton Substrate kit (Tropix; Applied Biosystems).

Migration and invasion assays in vitro

The 2D motility of cells was analyzed by recording phase-contrast or GFP fluorescence images with a multichannel time-lapse digital video microscope for several hours (Axiovert 200, 10×/0.25 NA plan Ph/VAR dry objective, HAL100 camera; incubation chamber at 37°C, 5% CO_2). Cell speed was determined by tracking cells with MetaMorph Software (Universal Imaging Corp.). The 3D morphology was analyzed by embedding tumor cells within a thick Matrigel matrix. After an 18-h incubation, cells were fixed in 4% paraformaldehyde and imaged by capturing at least 30 confocal sections of GFP fluorescence (SPI TCSNT confocal microscope [Leica]; Plan Apochromat 40×/1.3 NA oil objective; immersion oil #11513859 [Leica] with N_e = 1,518). These were subsequently reconstructed in 3D using Volocity software (Improvision). The 3D invasion assays were performed as previously described (Malliri et al., 1998). In brief, cells were allowed to attach to the underside (bottom) of the growth factor–depleted Matrigel-coated polycarbonate chambers (Transwells; 8-μm pore-size filters). The cells were then chemoattracted (10% FCS) across the filter and through the Matrigel above it. Cells were fixed in 4% paraformaldehyde, and GFP fluorescence was analyzed in z sections (one section every 4 μm) from the bottom of the filter, using a confocal microscope. 3D reconstructions of the GFP-expressing cells into the Matrigel were done using Volocity computer software. Cells were scored as amoeboid when the polarity index (long axis/short axis ratio) was less than two, with no apparent cellular protrusions.

In vivo imaging of tumor xenografts

10^6 tumor cells were injected subcutaneously into the flank of young adult immune-compromised mice. Once tumors were established (diam 4–7 mm), intravital imaging of tumor cell morphology and movement was performed on living anesthetized animals using two-photon microscopy, as described elsewhere (Sahai et al., 2005). The animal study protocols were conducted according to approved institutional guidelines for animal use. Tumors were fixed in 4% paraformaldehyde after imaging and stained for endomucin (details available on request) to reveal the presence of blood vessels.

Online supplemental material

Fig. S1 shows that Smurf1 does not interfere with SMAD or JNK activity in carcinoma cells. Fig. S2 shows the overall activity of downstream effectors of the Rho–ROCK pathway upon Smurf1 silencing. Fig. S3 shows

that Smurf1 silencing does not affect the vessel density in tumors. Video 1 shows a mesenchymal BE tumor cell moving in the tumor by extending a protrusion at the front. Video 2 shows rounded Smurf1-silenced BE tumor cells moving in the tumor with no protrusions, indicating that they are using the amoeboid mode of locomotion. Video 3 shows that mesenchymal BE tumor cells are not highly motile and that no tumor cells are seen in the vessels. Video 4 shows that amoeboid Smurf1-silenced BE tumor cells are highly motile and that many cells are visible in the vessels. Online supplemental material is available at http://www.jcb.org/cgi/content/full/jcb.200605135/DC1.

We thank Edurne Berra for providing us with the control shRNAs and siRNAs and for comments on the manuscript. We are grateful to Mike Olson for the gift of pLIMK and pMLC2 antibodies, and to Robert Grosse and Thomas Kitzing for the rhotekin-GFP reagents. We are grateful to Clare Watkins and Emma Nye for their technical assistance.

E. Vial is funded by the Association pour la Recherche sur le Cancer. E. Sahai is funded by Cancer Research UK.

Submitted: 22 May 2006
Accepted: 29 November 2006

References

Berra, E., E. Benizri, A. Ginouves, V. Volmat, D. Roux, and J. Pouyssegur. 2003. HIF prolyl-hydroxylase 2 is the key oxygen sensor setting low steady-state levels of HIF-1alpha in normoxia. *EMBO J.* 22:4082–4090.

Clark, E.A., T.R. Golub, E.S. Lander, and R.O. Hynes. 2000. Genomic analysis of metastasis reveals an essential role for RhoC. *Nature*. 406:532–535.

Cox, E.A., S.K. Sastry, and A. Huttenlocher. 2001. Integrin-mediated adhesion regulates cell polarity and membrane protrusion through the Rho family of GTPases. *Mol. Biol. Cell*. 12:265–277.

Croft, D.R., E. Sahai, G. Mavria, S. Li, J. Tsai, W.M. Lee, C.J. Marshall, and M.F. Olson. 2004. Conditional ROCK activation in vivo induces tumor cell dissemination and angiogenesis. *Cancer Res.* 64:8994–9001.

Friedl, P., and K. Wolf. 2003. Tumour-cell invasion and migration: diversity and escape mechanisms. *Nat. Rev. Cancer*. 3:362–374.

Goulimari, P., T.M. Kitzing, H. Knieling, D.T. Brandt, S. Offermanns, and R. Grosse. 2005. Galpha12/13 is essential for directed cell migration and localized Rho-Dia1 function. *J. Biol. Chem.* 280:42242–42251.

Hakem, A., O. Sanchez-Sweatman, A. You-Ten, G. Duncan, A. Wakeham, R. Khokha, and T.W. Mak. 2005. RhoC is dispensable for embryogenesis and tumor initiation but essential for metastasis. *Genes Dev.* 19:1974–1979.

Hall, A. 1998. Rho GTPases and the actin cytoskeleton. *Science*. 279:509–514.

Izzi, L., and L. Attisano. 2004. Regulation of the TGFbeta signalling pathway by ubiquitin-mediated degradation. *Oncogene*. 23:2071–2078.

Malliri, A., M. Symons, R.F. Hennigan, A.F. Hurlstone, R.F. Lamb, T. Wheeler, and B.W. Ozanne. 1998. The transcription factor AP-1 is required for EGF-induced activation of Rho-like GTPases, cytoskeletal rearrangements, motility, and in vitro invasion of A431 cells. *J. Cell Biol.* 143:1087–1099.

Ozdamar, B., R. Bose, M. Barrios-Rodiles, H.R. Wang, Y. Zhang, and J.L. Wrana. 2005. Regulation of the polarity protein Par6 by TGFbeta receptors controls epithelial cell plasticity. *Science*. 307:1603–1609.

Ridley, A.J. 2001. Rho GTPases and cell migration. *J. Cell Sci.* 114:2713–2722.

Sahai, E. 2005. Mechanisms of cancer cell invasion. *Curr. Opin. Genet. Dev.* 15:87–96.

Sahai, E., and C.J. Marshall. 2002. RHO-GTPases and cancer. *Nat. Rev. Cancer*. 2:133–142.

Sahai, E., and C.J. Marshall. 2003. Differing modes of tumour cell invasion have distinct requirements for Rho/ROCK signalling and extracellular proteolysis. *Nat. Cell Biol.* 5:711–719.

Sahai, E., and M.F. Olson. 2006. Purification of TAT-C3 exoenzyme. *Methods Enzymol.* 406:128–140.

Sahai, E., M.F. Olson, and C.J. Marshall. 2001. Cross-talk between Ras and Rho signalling pathways in transformation favours proliferation and increased motility. *EMBO J.* 20:755–766.

Sahai, E., J. Wyckoff, U. Philippar, J.E. Segall, F. Gertler, and J. Condeelis. 2005. Simultaneous imaging of GFP, CFP and collagen in tumors in vivo using multiphoton microscopy. *BMC Biotechnol.* 5:14.

Suzuki, C., G. Murakami, M. Fukuchi, T. Shimanuki, Y. Shikauchi, T. Imamura, and K. Miyazono. 2002. Smurf1 regulates the inhibitory activity of Smad7 by targeting Smad7 to the plasma membrane. *J. Biol. Chem.* 277:39919–39925.

van de Wetering, M., I. Oving, V. Muncan, M.T. Pon Fong, H. Brantjes, D. van Leenen, F.C. Holstege, T.R. Brummelkamp, R. Agami, and H. Clevers. 2003. Specific inhibition of gene expression using a stably integrated, inducible small-interfering-RNA vector. *EMBO Rep.* 4:609–615.

Vial, E., E. Sahai, and C.J. Marshall. 2003. ERK-MAPK signaling coordinately regulates activity of Rac1 and RhoA for tumor cell motility. *Cancer Cell*. 4:67–79.

Wang, H.R., Y. Zhang, B. Ozdamar, A.A. Ogunjimi, E. Alexandrova, G.H. Thomsen, and J.L. Wrana. 2003. Regulation of cell polarity and protrusion formation by targeting RhoA for degradation. *Science*. 302:1775–1779.

Wang, W., J.B. Wyckoff, V.C. Frohlich, Y. Oleynikov, S. Huttelmaier, J. Zavadil, L. Cermak, E.P. Bottinger, R.H. Singer, J.G. White, et al. 2002. Single cell behavior in metastatic primary mammary tumors correlated with gene expression patterns revealed by molecular profiling. *Cancer Res.* 62:6278–6288.

Wilkinson, S., H.F. Paterson, and C.J. Marshall. 2005. Cdc42-MRCK and Rho-ROCK signalling cooperate in myosin phosphorylation and cell invasion. *Nat. Cell Biol.* 7:255–261.

Worthylake, R.A., and K. Burridge. 2003. RhoA and ROCK promote migration by limiting membrane protrusions. *J. Biol. Chem.* 278:13578–13584.

Wyckoff, J.B., S.E. Pinner, S. Gschmeissner, J.S. Condeelis, and E. Sahai. 2006. ROCK- and myosin-dependent matrix deformation enables protease-independent tumor-cell invasion in vivo. *Curr. Biol.* 16:1515–1523.

Yamashita, M., S.X. Ying, G.M. Zhang, C. Li, S.Y. Cheng, C.X. Deng, and Y.E. Zhang. 2005. Ubiquitin ligase Smurf1 controls osteoblast activity and bone homeostasis by targeting MEKK2 for degradation. *Cell*. 121:101–113.